 doi:10.20944/preprints202103.0244.v1

Analysis of Land Surface Temperature due to Dynamics of Green Spaces and Water bodies using Geospatial Techniques in Gida Kiremu, Limu and Amuru Districts, Western Ethiopia

Authors Information

[1*]Mitiku Badasa Moisa, [2]Lachisa Busha Hinkosa

[1*]Department of Agricultural Engineering, Faculty of Technology, Wollega University Shambu campus

Email: mitikubadasa10@gmail.com

[2]Department of Agricultural Engineering, Faculty of Technology, Wollega University Shambu campus

Email: latibu85@gmail.com

*Corresponding author e-mail: mitikubadasa10@gmail.com

Abstract

Analysis of the correlation between indices (Normalized Difference Vegetation Index, Normalized Difference Barren Index and Modified Normalized Difference Water Index) and land surface temperature is used to natural resources and environmental studies. This research aimed to analysis of Land Surface Temperature due to dynamics of Different Indices (NDVI, NDBaI and MNDWI) Using Remote Sensing Data in three selected districts (Gida Kiremu, Limu and Amuru), western Ethiopia. From thermal and multispectral bands of landsat imageries (Landsat TM of 1990, landsat ETM+ of 2003 and landsat OLI/TIRS of 2020) Land surface temperature and NDVI, NDBaI and MNDWI were calculated. Correlation analysis was used to indicate relationships between LST with NDVI, NDBaI and MNDWI. The study found that Land Surface Temperature was increased by 5^0C from 1990 to 2020. Vegetation areas (NDVI) and Water bodies (MNDWI) have strong negative relationship with Land Surface Temperature (R^2= 0.99, 0.95) whereas Barren land (NDBaI) has positive relationship with Land Surface Temperature (R^2= 0.96). Finally, we recommend the decision makers and environmental analyst to emphasis the importance of vegetation cover and water body to minimize the potential impacts of land surface temperature.

Keywords: Land surface temperature (LST), NDVI, NDBaI, MNDWI, Satellite data

Introduction

Most of human actions are the main cause for constantly declining the vegetation cover of the earth's surface (Sahana *et al.,* 2016). The decrements of vegetation cover the cause for the increment of land surface temperature. Land surface temperature (LST) defined as skin temperature of the earth's temperature is a key factor for land surface processing studies at both a regional and global scale (Thanh *et al.,* 2018). According to Alemu (2019) stated that land surface temperature is calculated from emitted energy by earth surface or satellite based devices. Relationships of land surface temperatures with Normalized Difference Index, Normalized

 doi:10.20944/preprints202103.0244.v1

Barren Index and Modified Normalized Difference Water Index were examined (Qinqin, 2012). Analysis of spatial changeability of Normalized Difference Vegetation Index (NDVI), Land Surface Temperature (LST) the nexus between the factors is essential in natural and environmental studies (Zareie *et al.,* 2016) as well as for spatial decision making and for monitoring of the natural resources. Furthermore, the investigation of Land surface temperature with NDVI, NDBaI and MNDWI of different times can be used to identify land use/land cover changes, which were made because of the forest fires, deforestation, built up expansion, expansion of agricultural land and grazing land restoration (Zhou and Wang, 2011; Mimbrero *et al.,* 2014). Remote sensing indices are employed to quantitatively represent land use/land cover types. For example, the NDVI has been used to confirm the role of green space (Yuan and Bauer, 2007). The Normalized Difference Barren Index (NDBaI) and Modified Normalized Difference Water Index (MNDWI) have been employed to represent degraded land and water areas quantitatively (Gao, 1996; Zha *et al*., 2003). Though previous studies have been adopted these indices to model Land Surface Temperature (LST) (Chen *et al.,* 2016), only a few of them have compared the modeling results of different years. The study area was experienced increasing Land Surface Temperature (LST) due to degradation of vegetation cover and blue spaces. Therefore, this study attempted to analysis of Spatiotemporal Land Surface Temperature in Relative to Different Indices (NDVI, NDBaI and MNDWI) using Geospatial Techniques in three selected districts (Gida Kiremu, Limu and Amuru), western Ethiopia.

Materials and Methods

Description of the study area

This research conducted in selected woreda was located in East Wollega zone and Horo Guduru Wollega zone. Geographically the study area was lies between $9^0 27' 00''$ and $10^0 18' 00''$ N and $36^0 19' 30''$ and $37^0 10' 30''$ E. Administratively, Amuru district is located in Horo Guduru Wollega Zone and Gida kiremu and Limu districts were located in East Wollega Zone of Oromia National Regional State in Western Ethiopia (Figure 1). The altitude of the study area lies between 2496.61m and 713.32m above mean sea level. It covers an area of about 5086.65km^2.

Preprints (www.preprints.org) | NOT PEER-REVIEWED | Posted: 9 March 2021 doi:10.20944/preprints202103.0244.v1

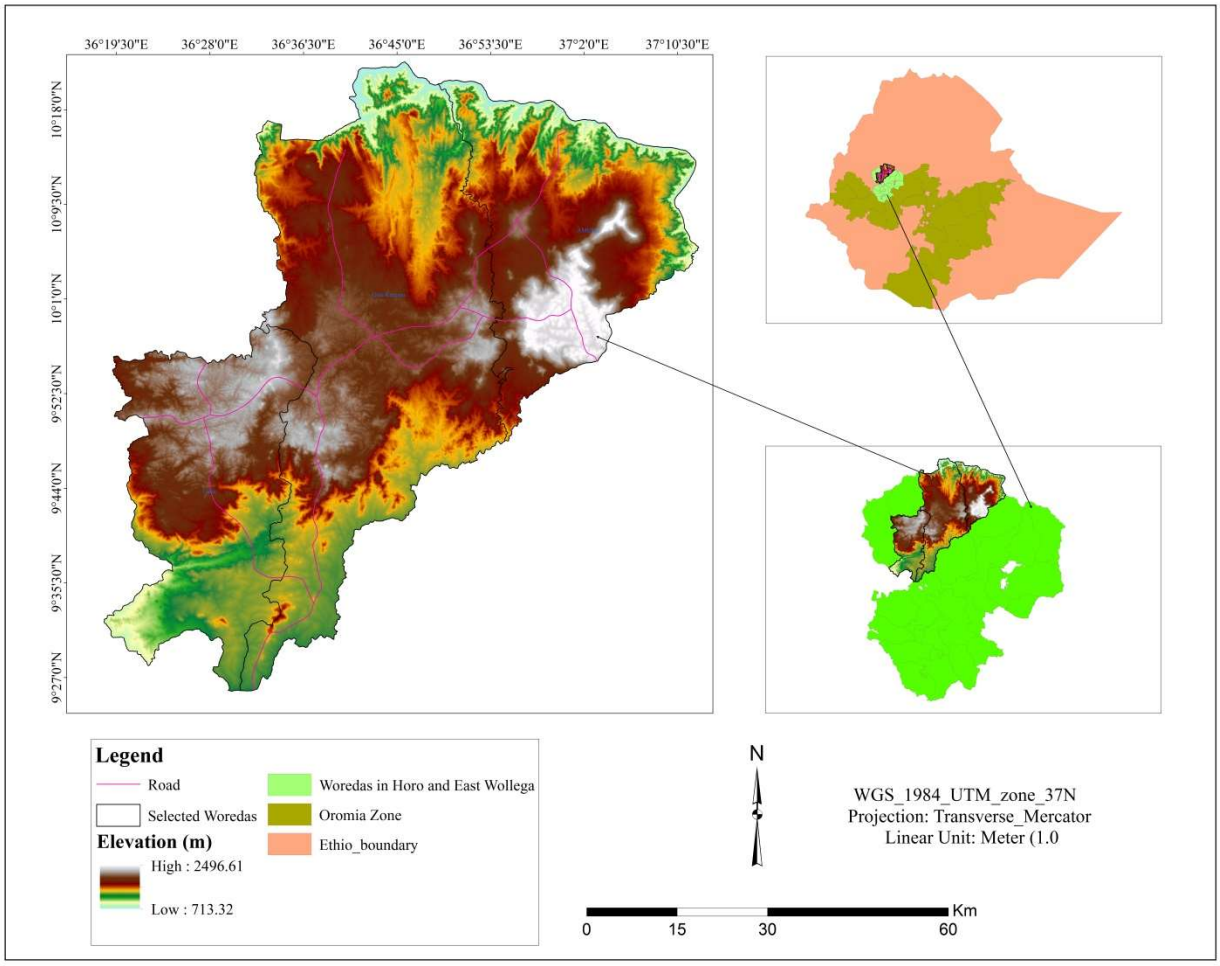

Figure 1: Location map of the study area

Types of data and Descriptions

Three different years of landsat imageries were used for this study. Thermal and multispectral bands of landsat TM of 1990, landsat ETM+ of 2003 and landsat OLI/TIRS of 2020 were downloaded from USGS (http://earthexplorer. usgs.gov/) free of cost. The detail information of these data were presented in (Table 1)

Table 1: Remote sensing data used for the study

Satellite Image	Path/Row	Sensor	Resolution (m)	No of bands	Date of Acquisitions
Landsat 5	170/53	TM	30	7	12-01-1990
Landsat 7	170/53	ETM+	30	7	20-02-2003
Landsat 8	170/53	OLI/TIRS	30	11	11-02-2020

Preprints (www.preprints.org) | NOT PEER-REVIEWED | Posted: 9 March 2021 doi:10.20944/preprints202103.0244.v1

Method of data analysis

In this study, calculation of land surface temperature and Normalized Difference Vegetation Index, Modified Normalized Difference Water Index, Normalized Difference Barren Index. For general information methodological flow diagram of the study was presented in (Figure 2).

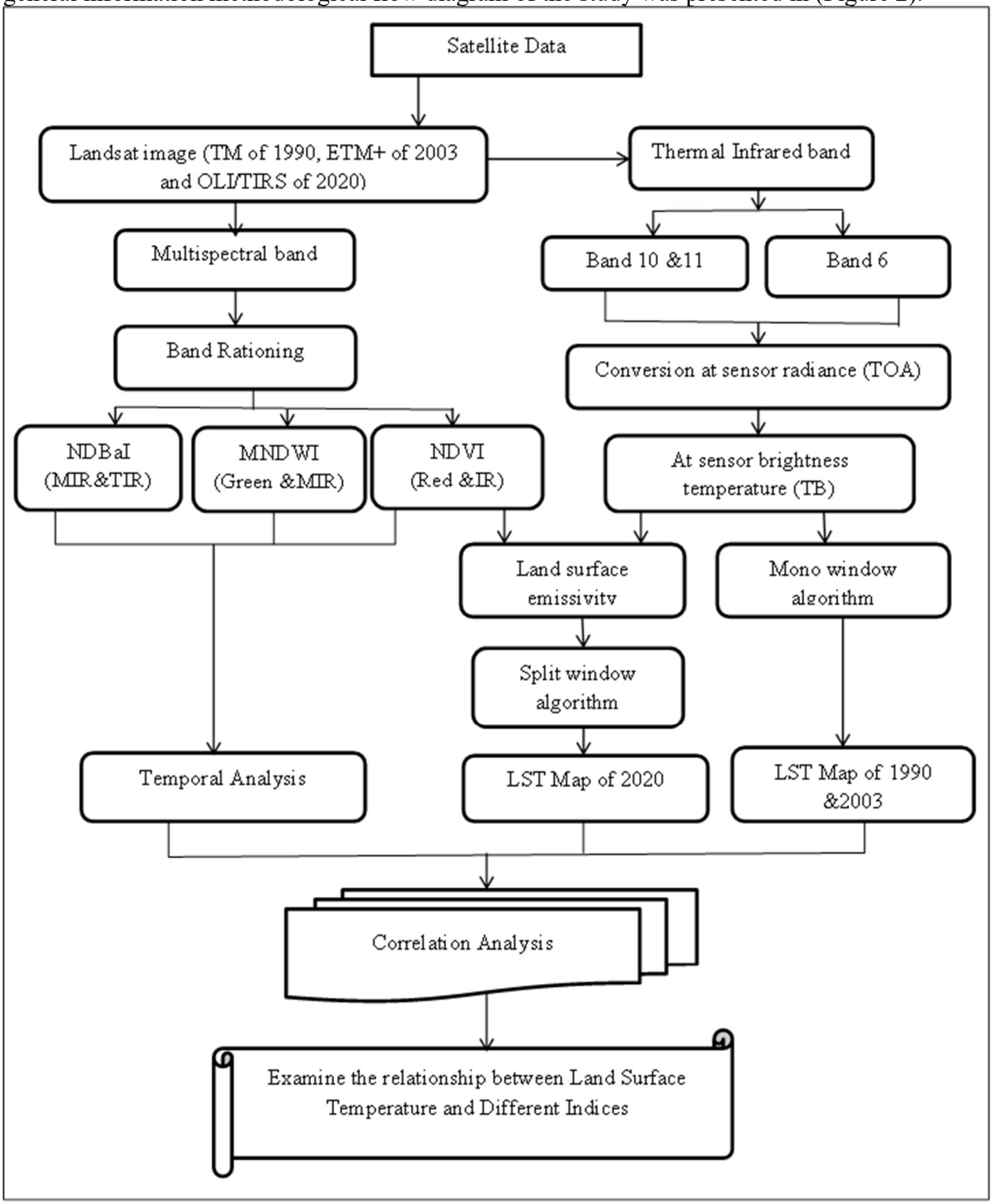

Figure 2: Methodological flowchart of the study

Preprints (www.preprints.org) | NOT PEER-REVIEWED | Posted: 9 March 2021 doi:10.20944/preprints202103.0244.v1

Vegetation covers (NDVI)

This index is used to estimate the amount of vegetation cover on the earth surface. This NDVI was calculated from multi spectral bands of landsat images of all study period. Band 4 for landsat 5 &7, band 5 for landsat 8 used to measure near infrared bands. As well as band 3 for landsat 5&7, band 4 for landsat 8 was used to measure red bands of the landsat data. The formula of this index presented in (Eq 1)

$$NDVI = \frac{Red-NIR}{Red+NIR} \qquad \textbf{(Eq 1)}$$

The NDVI values ranges between -1.0 and 1.0. The NDVI values for health and dense vegetation always ranges between 0.2 and 0.9 (Bustos and Meza, 2015). Whereas, vegetation such as rock, water and barren lands indicated by the values less than 0.1 (Fu and Burger, 2015)

Modified Normalized Difference Water Index (MNDWI)

The MNDWI is designated to represent water areas often reveal remarkable differences in thermal characteristics when modeling thermal environment (Xu, 2008; Zhifeng and Jianjun, 2012). It calculated from the measurements of green band (band 2 for landsat 5 & 7, band 3 for landsat 8) and middle infrared (band 5 for landsat 5 & 7, band6 for landsat 8) reflectance the formula (Eq 2).

$$MNDWI = \frac{Green-MIR}{Green+MIR} \qquad \textbf{(Eq 2)}$$

Normalized Difference Barren Index (NDBaI)

The NDBaI is selected to represent barren land areas often indicate significant differences in thermal characteristics when predicting thermal environment (Zhifeng and Jianjun, 2012). It calculated from the middle infrared (band 5 for landsat 5 and 7, band6 for landsat 8) and thermal infrared (band 6 for landsat 5 and 7, band 10 and 11 for landsat 8) reflectance, calculated by formula (Eq 3).

$$NDBaI = \frac{MIR-TIR}{MIR+TIR} \qquad \textbf{(Eq 3)}$$

Retrieval of Land Surface Temperature (LST)

Land surface temperatures (LST) developed from Landsat ETM+ and OLI/TIRS data, including mono window algorithm (Qin *et al*., 2001), single channel and split window algorithm (Jimenez and Sobrino, 2003). Split window algorithm was used to retrieve LST from Landsat 8 data that has two bands (Band 10 and Band 11). It uses brightness temperature of the two bands of Thermal Infrared (TIR), mean and difference in land surface emissivity for estimating LST (Cheng *et al*., 2015).

Step I: **Conversion of DN in to Radiance**

A. Mono Window Algorithm

In Mono window algorithm digital numbers are converted to at-sensor radiances sensor, before to calculate brightness temperature.

The ETM+ DN values ranges between 0 and 255 (Eq.4).

$$L\lambda = \frac{LMAX\lambda-LMIN\lambda}{QCALMAX-QCALMIN} x\,(DN - QCALMIN) + LMIN\lambda \qquad \textbf{(Eq.4)}$$

Where:

QCLA = is the quantized calibrated pixel value in Digital Number (DN)

QCAL= is the quantized calibrated pixel value in Digital Number (DN)

Preprints (www.preprints.org) | NOT PEER-REVIEWED | Posted: 9 March 2021 doi:10.20944/preprints202103.0244.v1

LMINλ= is the spectral radiance that is scaled to QCALMIN in watts/(meter squared*ster* μm)
LMAXλ= is the spectral radiance that is scaled to QCALMAX in watts/(meter squared*ster* μm)
QCALMIN= is the minimum quantized calibrated pixel value corresponding to LMINλ in DN
QCALMAX= is the maximum quantized calibrated pixel value corresponding to LMAXλ in DN= 255

B. Split window algorithm

The split window algorithm (SWA) is used for Landsat 8 LST estimation as previously used by various scholars (Aik *et al*., 2020; Sahana *et al*., 2016; Atitar and Sobrino, 2009). The Digital Numbers (DNs) of bands 10 and 11 from the Landsat 8 OLI was first converted to spectral radiance (Eq.5.

$$\boldsymbol{L\lambda = (ML * QCal) + AL} \qquad \textbf{(Eq.5)}$$

Where;
$L\lambda$ is Top of Atmosphere (TOA) spectral radiance (Wm^{-2} sr^{-1} μm^{-1})
ML is Band-specific multiplicative rescaling factor from the metadata (RADIANCE_MULT_BAND x, where x is the band number)
AL is Band-specific additive rescaling factor from the metadata (RADIANCE_ADD_BAND_x, where x is the band number)
QCal is Quantized and calibrated standard product pixel values (DN)

Step II. Conversion to Temperature (ETM^+)

The mono-window algorithm is used to calculate LST based on land surface emissivity, atmospheric trans-emissivity, brightness temperature, and average atmospheric temperature (Zhang *et al*., 2006).
TM and ETM+ Band 6 imagery can also be converted from spectral radiance (as described above) to a more physically useful variable (Eq.6). The conversion formula is:

$$\mathbf{T} = \frac{\boldsymbol{K2}}{\boldsymbol{ln}\left(\frac{\boldsymbol{K1}}{\boldsymbol{L\lambda}}+\mathbf{1}\right)} \qquad \textbf{(Eq.6)}$$

T = Effective at-satellite temperature in Kelvin
K2 = Calibration constant 2
K1 = Calibration constant 1
L = Spectral radiance in watts/(meter squared * ster * μm)

The split-window algorithm (SW) was applied to calculate LST for this study. Due to the significant reliability of the SW algorithm, it has a wider applicability. It uses the brightness temperatures of two TIR bands (band 10 and band 11 of Landsat-8) to calculate mean land surface emissivity, and then to estimate LST.

TB10 is brightness temperature of band 10 (Kelvin K);
TB11 is brightness temperature of band 11 (Kelvin K);
Ɛ is mean value of Land Surface Emissivity (LSE) of TIR bands;
W is content of water vapors in the atmosphere;
ΔƐ is difference between LSE of bands 10 and 11.e emissivity, difference of land surface emissivity, and then to estimate LST (Eq.7):

$$\mathbf{BT} = \frac{\boldsymbol{K2}}{\mathbf{ln}\left(\frac{\boldsymbol{K1}}{\boldsymbol{L\lambda}}+\mathbf{1}\right)} \qquad \text{(Eq.7)}$$

Where;

Preprints (www.preprints.org) | NOT PEER-REVIEWED | Posted: 9 March 2021 doi:10.20944/preprints202103.0244.v1

***BT*:** is effective at-sensor brightness temperature (K);
K2: is calibration constant 2 (K);
***K1*:** is calibration constant 1 (W/ (m^2 * sr * μm));
Lλ: is spectral radiance at the sensor's aperture (W/ (m^2 * sr * μm)); and
Ln: is natural logarithm

Step III: Land surface Emissivity Estimation
According to Sobrino *et al*. (2004), the emissivity is calculated using (Eq.9)

$$\boldsymbol{\varepsilon = 0.004 * PV + 0.986} \quad \text{(Eq.8)}$$

Where PV is the vegetation proportion obtained according to
Carlson and Ripley formula (Eq.10);

$$\mathbf{PV} = \left[\frac{\mathbf{NDVI - NDVImin}}{\mathbf{NDVImax - NDVImin}}\right]^{\mathbf{2}} \quad \text{(Eq.9)}$$

The calculated radiant surface temperatures will be corrected for emissivity using the equation (Eq.11):

$$\mathbf{LST} = \frac{\mathbf{TB}}{\mathbf{1 + \left(\lambda \frac{TB}{P}\right) In\varepsilon}} \quad \text{(Eq.10)}$$

Where;
LST: land surface temperature (in Kelvin);
TB: radiant surface temperature (in Kelvin)
***λ*:** the wavelength of emitted radiance (11.5 μm).
***ρ*:** h×c/σ (1.438 $\times 10^{-2}$ mK); h is Planck's constant (6.26×10−^{34} J s); c is the velocity of light (2.998 $\times 10^{8}$ m/s); σ is Stefan Boltzmann's constant (1.38×10−^{23}J K^{-1}); and ε is land surface emissivity.

Finally, land surface temperature results from Landsat ETM+ and OLI/TIRS was converted into degree Celsius, by subtracting 273.15. To convert temperature the degree Kelvin (^{0}K) to degree Celsius (^{0}C), (Eq 11) was used.

$$\boldsymbol{0C = 0K - 273.15} \quad \text{(Eq 11)}$$

Where: ^{0}C = LST result in degree Celsius;

^{0}K = LST result in degree Kelvin

Result and Discussion
Analysis of Land Surface Temperature (LST)

Spatial pattern of Land surface temperature was calculated for the year of 1990, 2003 and 2020 of the study area respectively. The result indicated that Northeastern and Southwestern part of the study area shows high land surface temperature (LST) in all selected year (Figure 3). Because declined green space (vegetation cover) and increasing of barren land. Beside eastern, central and western part of the study area shows that low land surface temperature (LST), because of high vegetation cover.

Preprints (www.preprints.org) | NOT PEER-REVIEWED | Posted: 9 March 2021 doi:10.20944/preprints202103.0244.v1

Gradually, LST was increased in all selected year the mean of 23.70C in 1990, 24.30C in 2003 and 28.70C in 2020. The average temperatures rise from 1990-2020 by 5^0C this increment is between 30 years. According to Rasul *et al.* (2012) during the 20th century, they estimate the temperature will increase further between 1.4^0C and 5.8^0C by 2100 year.

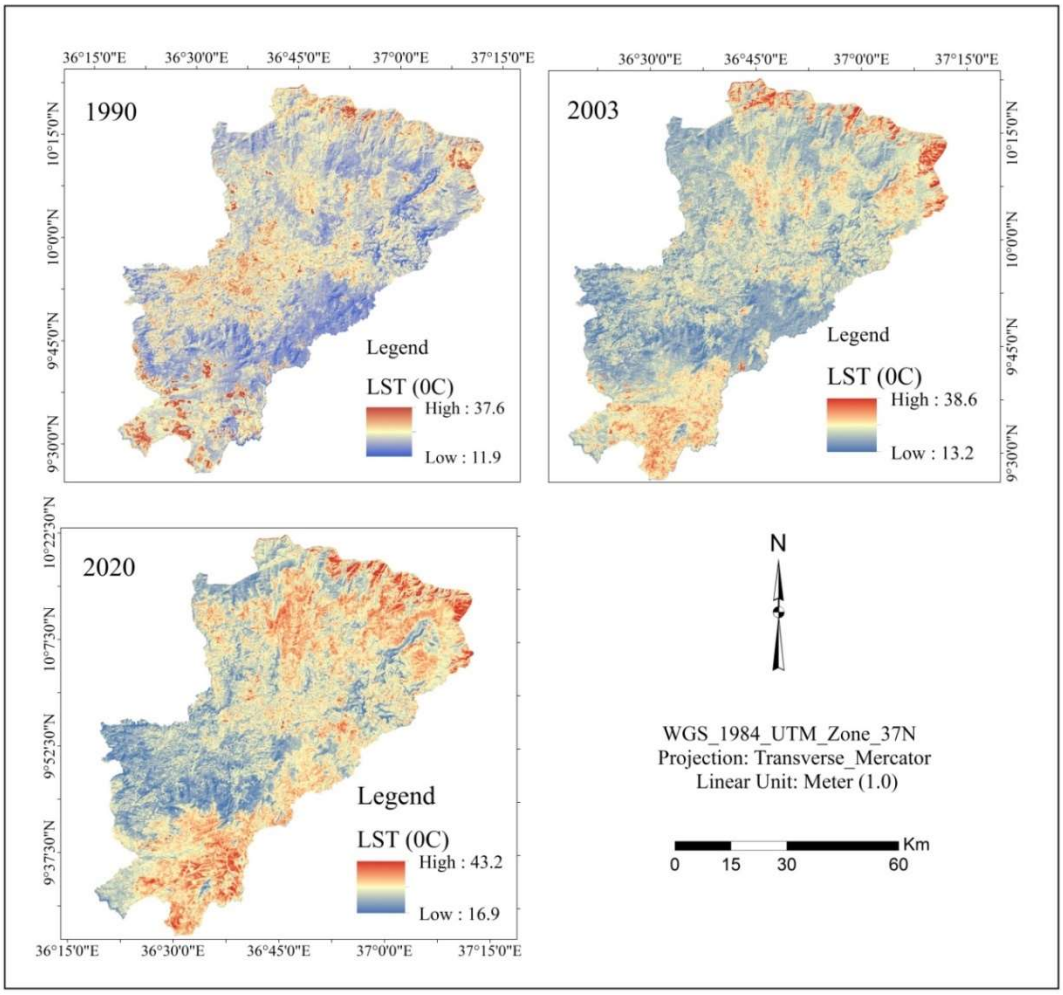

Figure 3: LST map of the study area

Analysis of relationship between Land Surface Temperature (LST) and Different Indices
Analysis of the correlation between (LST) and (NDVI)

The correlation between vegetation cover (NDVI) and Land Surface Temperature (LST) of the study area was presented in Figures, Tables and graphs. Regarding the first part, (Figure 4) determine the distribution of Vegetation cover (NDVI) respectively.

Preprints (www.preprints.org) | NOT PEER-REVIEWED | Posted: 9 March 2021 doi:10.20944/preprints202103.0244.v1

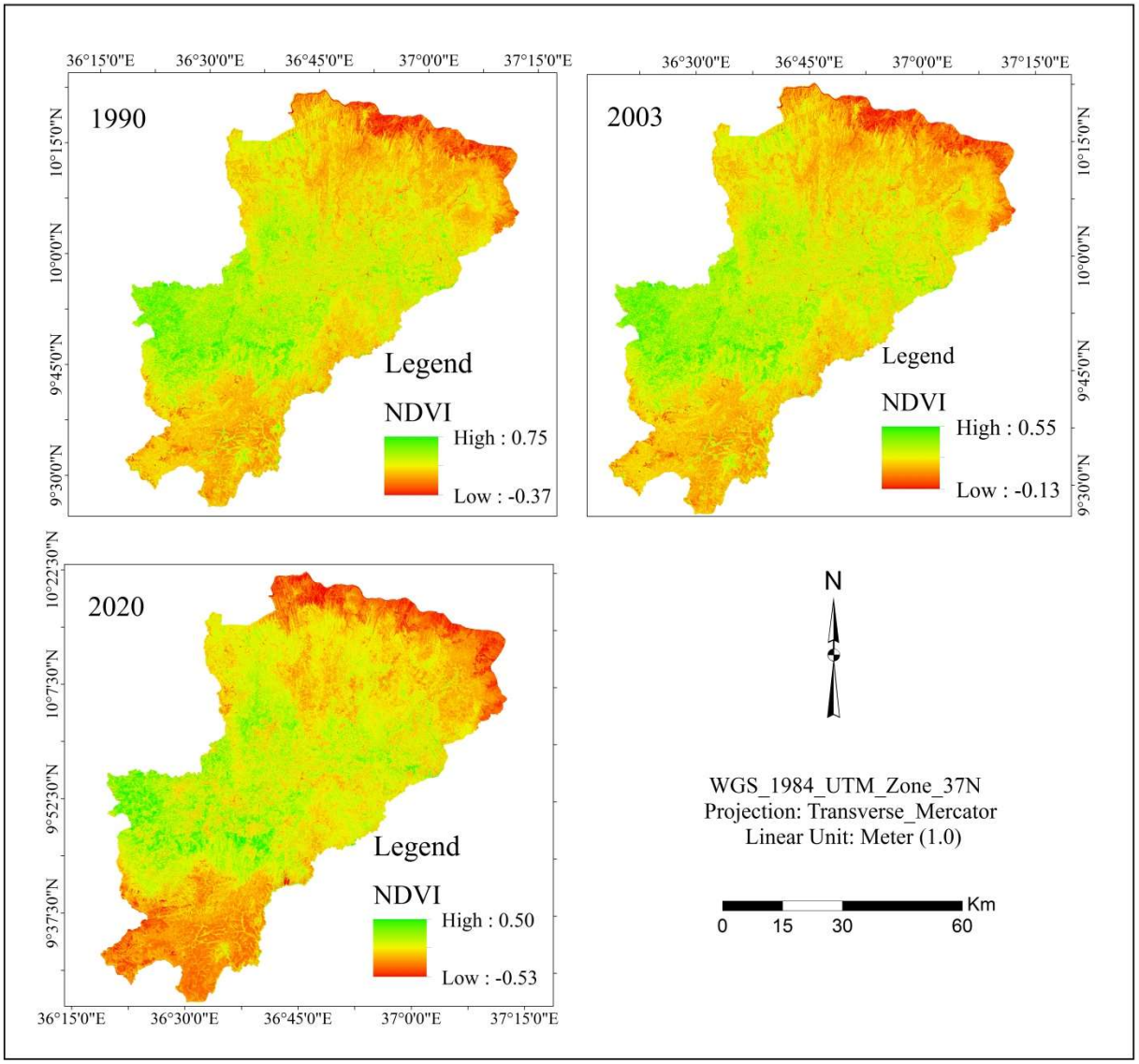

Figure 4: Normalized Difference Vegetation Index map of the study area

(Table 2 and Figure 5) demonstrate the relationship between the two parameters in 2020. It is found that LST values range with maximum temperature (43.2^0C) to minimum temperature (16.9^0C) while the NDVI values ranges between 0.50 to -0.53 maximum to minimum respectively.

The result indicates that LST and NDVI have negative strong relationship with (R^2= 0.99). It reveals that High land surface temperature more related with low green spaces (vegetation cover) and vice versa. The result is agreement with (Abhijit *et al.,* 2018; Alemu, 2019; Wedajo *et al.,* 2019).

Preprints (www.preprints.org) | NOT PEER-REVIEWED | Posted: 9 March 2021 doi:10.20944/preprints202103.0244.v1

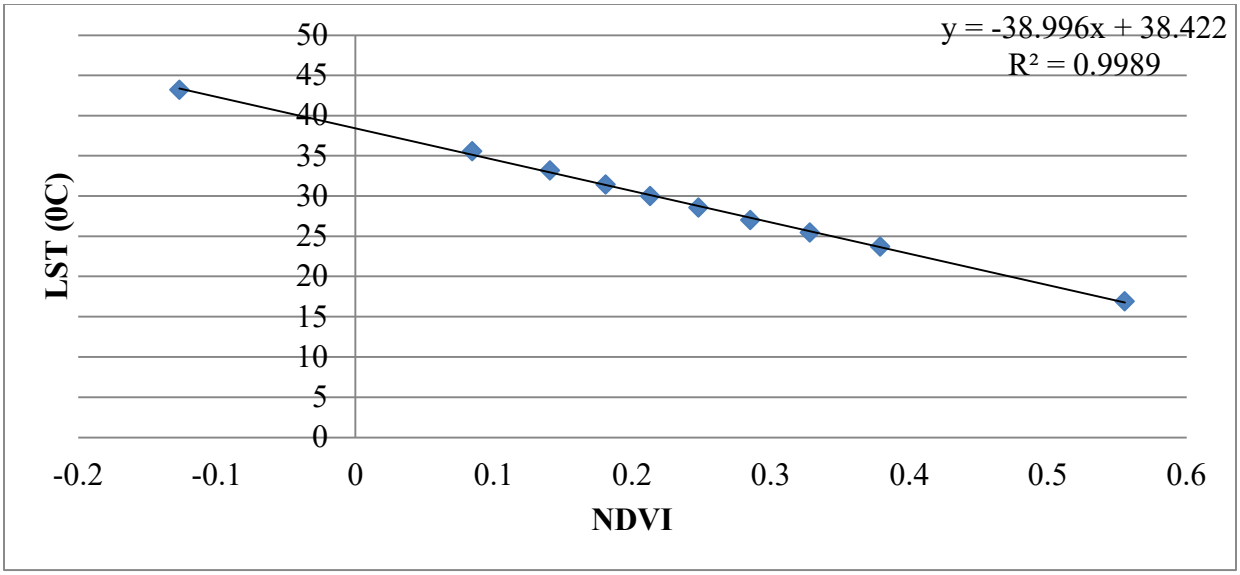

Figure 5: Relationship of LST and NDVI of study area

The correlation between (LST) and (NDBaI)

The result shows that LST and NDBaI have positive strong relationship with (R^2= 0.96). It shows that high land surface temperature exist in degraded land or barren land which has high value of NDBaI (Figure 6). The correlation of two parameters presented in (Figure 7). The result in line with (Zhifeng and Jianjun, 2012)

Preprints (www.preprints.org) | NOT PEER-REVIEWED | Posted: 9 March 2021 doi:10.20944/preprints202103.0244.v1

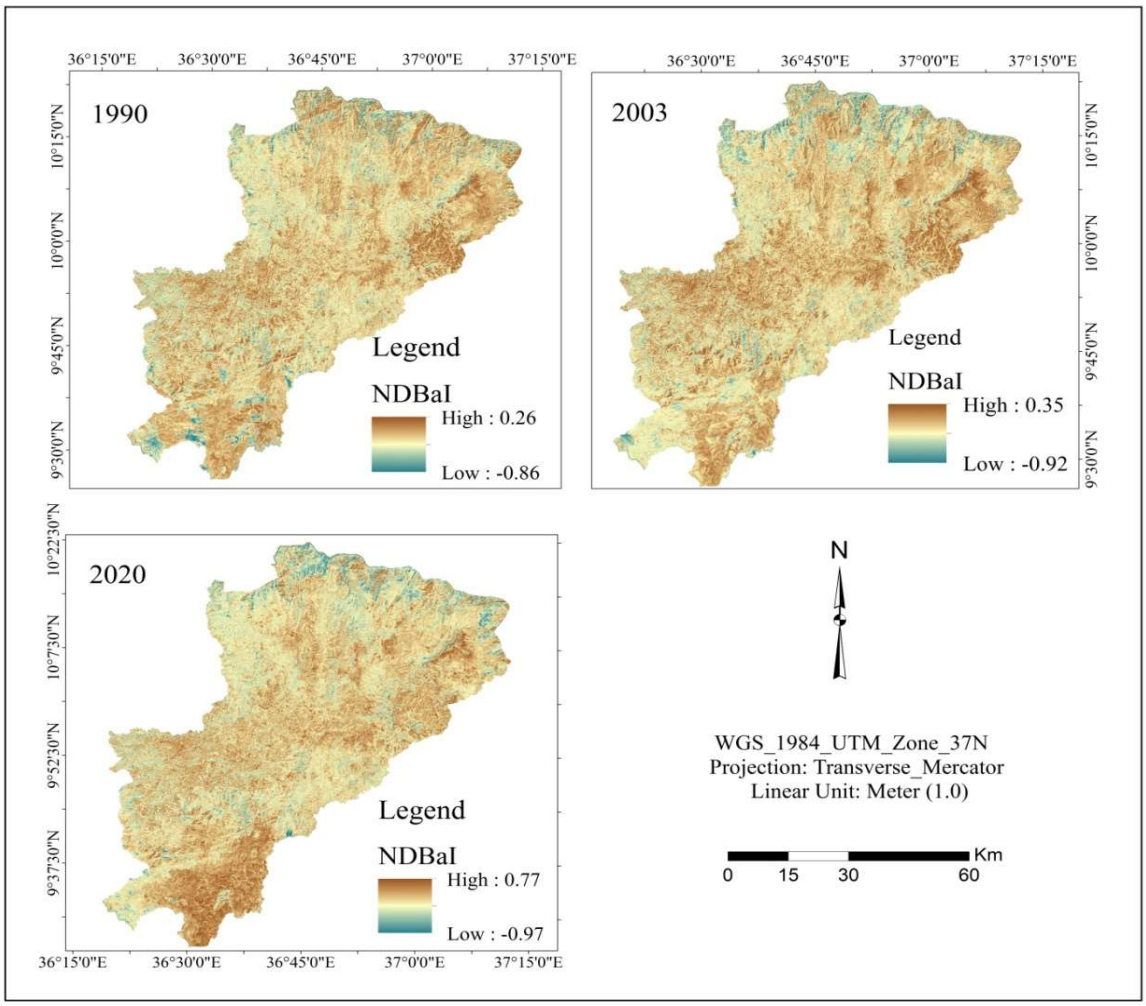

Figure 6: Normalized Difference Barren Index (NDBaI) map of the study area

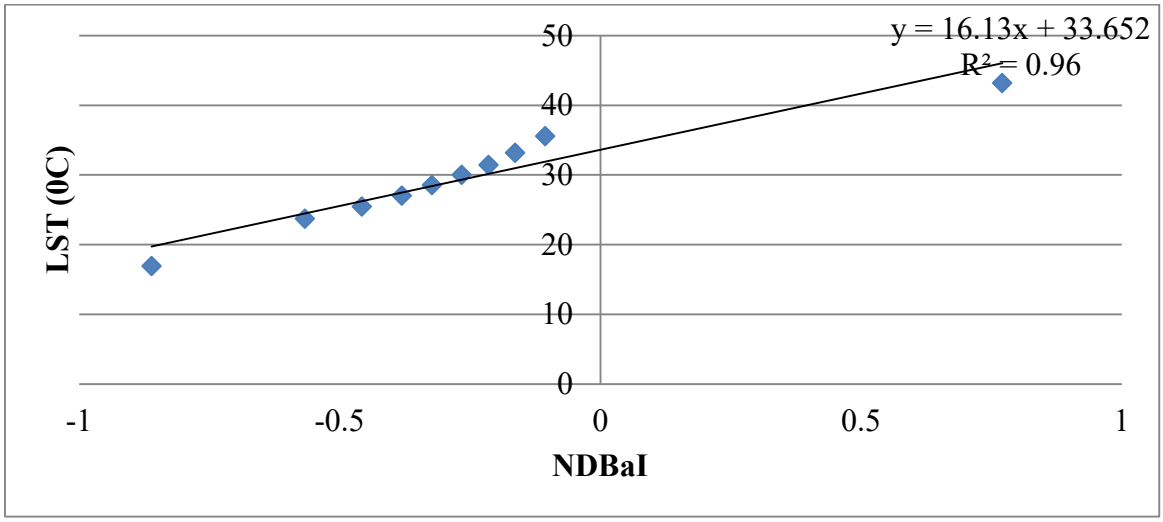

Figure 7: Relationship of LST and NDBaI of study area

Preprints (www.preprints.org) | NOT PEER-REVIEWED | Posted: 9 March 2021 doi:10.20944/preprints202103.0244.v1

Correlation between LST and MNDWI

The correlation of two parameters computed from landsat 8 of 2020. The result reveals that LST and MNDWI have negative strong relationship with coefficient determination of (R2= 0.95). Northern and southern part of the study area has high MNDWI (Figure 8).

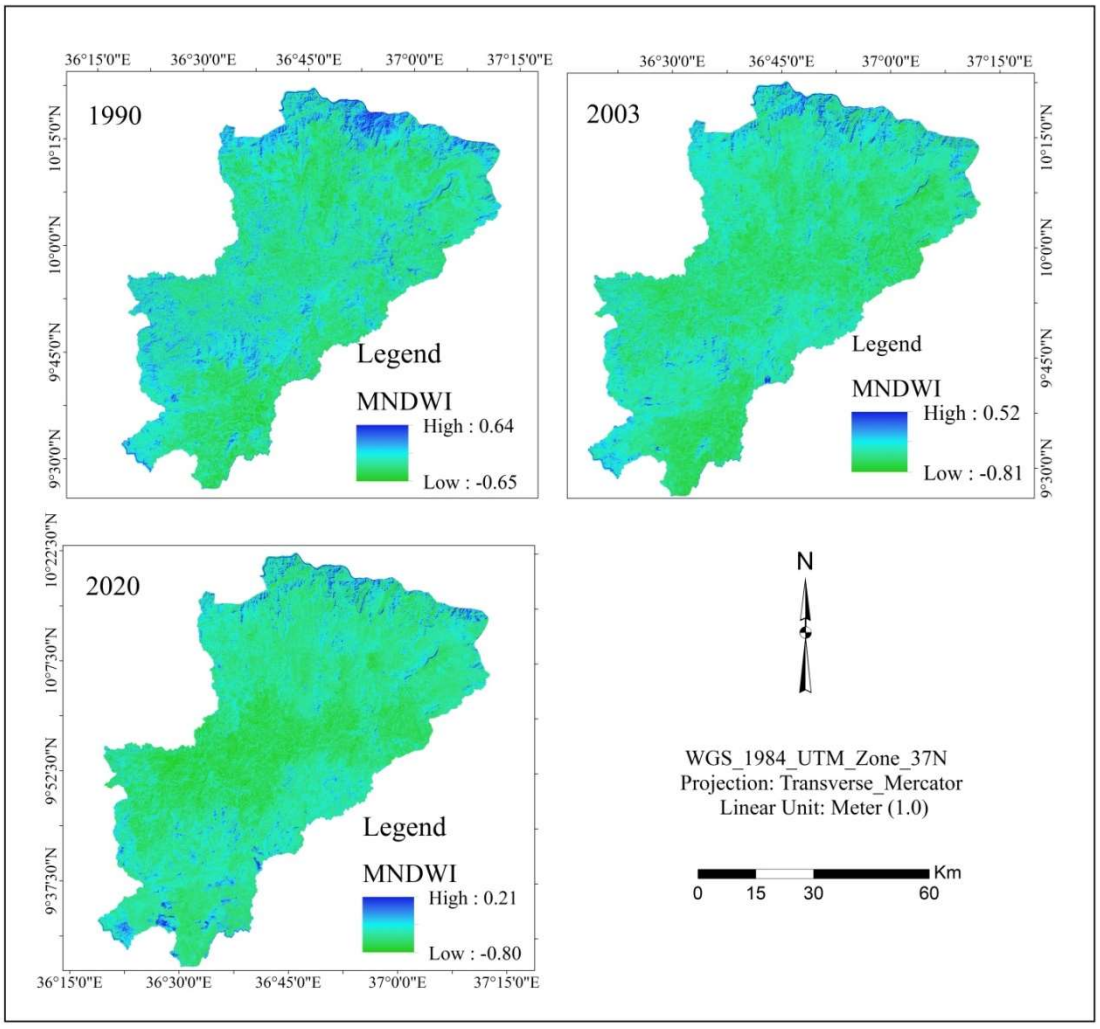

Figure 8: Modified Normalized Difference Water Index (MNDWI) map of the study area

The result shows high land surface temperature more recorded in low water areas. The correlation of LST and MNDWI were presented in (Figure 9). The result is in agreement with (Zhou and Wang, 2011; Zhifeng and Jianjun, 2012).

Preprints (www.preprints.org) | NOT PEER-REVIEWED | Posted: 9 March 2021 doi:10.20944/preprints202103.0244.v1

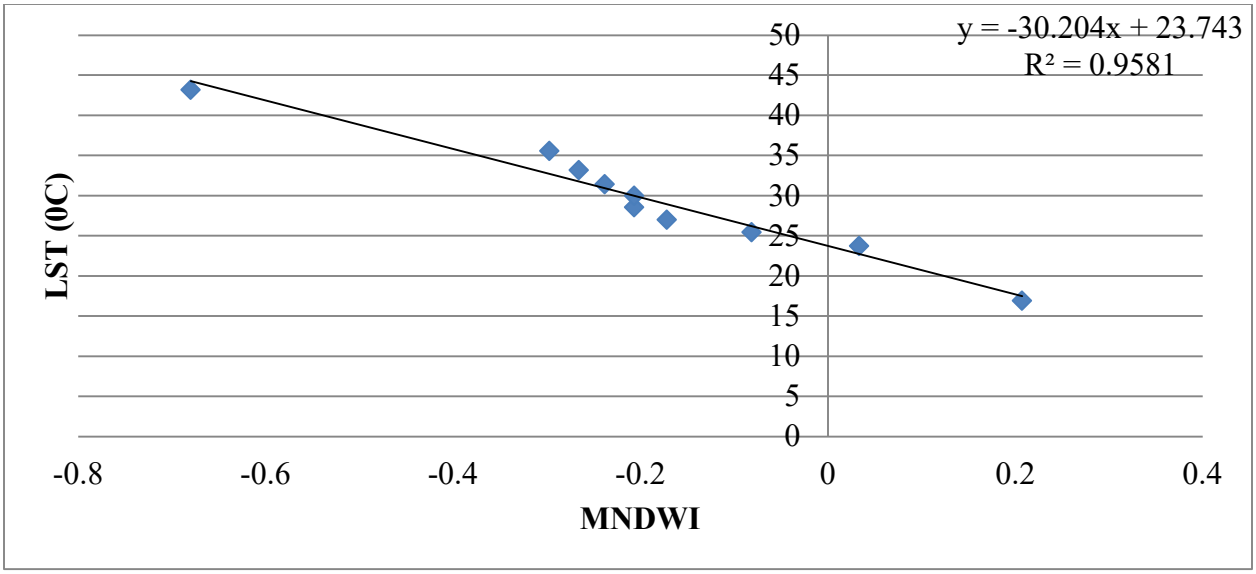

Figure 9: Relationship of LST and MNDWI of study area

Generally, the relations of all parameters were presented in (Table 2). Land surface temperature has direct relationship with Normalized Difference Barren Index (NDBaI) while LST has indirect relationship with NDVI and MNDWI.

Table 2: Correlation between LST, NDVI, NDBaI and MNDWI

correlation	*LST*	*NDBaI*	*NDVI*	*MNDWI*
LST	1			
NDBaI	0.95767*	1		
NDVI	-0.9995*	-0.9627*	1	
MNDWI	-0.9581*	-0.979*	0.98452*	1

*shows that Correlation values between them

Conclusion

In this paper, evaluation of Spatiotemporal Land Surface Temperature in Relation to different indices (NDVI, NDBaI and MNDWI) Using Remote Sensing Data in three selected districts (Gida Kiremu, Limu and Amuru), western Ethiopia. The study investigates the effect of changes in different indices (NDVI,NDBaI and MNDWI) over LST of the study area. Land surface temperature was increased by 5^0C from 1990 to 2020. The study found that the vegetation area (NDVI) and Water bodies (MNDWI) have a strong negative relatinship with land surface temperature, whereas Barren land (NDBaI) have positive relationship with land surface temperature.

Lists of abbreviations

LST	Land Surface Temperature
NDVI	Normalized Difference Vegetation Index
MNDWI	Modified Normalized Difference Water Index
NDBaI	Normalized Difference Barren Index
TM	Thematic Mapper
ETM+	Enhanced Thematic Mapper plus
OLI/TIRS	Operational Land Imager/Thermal Infrared Sensor

Declarations

Consent for publication: The authors agreed to publish the manuscript on Climate

Availability of data: Available in this manuscript

Competing interest: The authors declared no competing interest

Funding: No funding received for this research

Author contributions

MBM involved in research design, data collection, data analysis, and draft manuscript. LBH involved in data analysis. MBM also participated in methodology, data analysis and manuscript edition. All authors read and approved the final manuscript.

Acknowledgments

The authors would like to acknowledge Wollega University Shambu Campus Faculty of Technology for the existing facilities to conduct this research.

References

Abhijit S Patil , S S Panhalkar , Sabiha B , Shanishwar B (2018) Impact of Land use Land Cover Change on Land Surface Temperature using Geo-informatics Techniques. *International Journal of Research and Analytical Reviews* (IJRAR) www.ijrar.org

Aik DHJ, Ismail MH, and Muharam FM (2020) Land Use/Land Cover Changes and the Relationship with Land Surface Temperature Using Landsat and MODIS Imageries in Cameron Highlands, Malaysia. *Land*. 9, 372.

Alemu MM (2019) Analysis of Spatio-temporal Land Surface Temperature and Normalized Difference Vegetation Index Changes in the Andassa Watershed, Blue Nile Basin, Ethiopia. *J. Resour. Ecol*. 10(1): 77-85 DOI: 10.5814/j.issn.1674-764x.2019.01.010 www.jorae.cn

Atitar M, and Sobrino J, (2009) A split-window algorithm for estimating LST from meteosat 9 data: Test and comparision with data and MODIS LSTs. IEEE Geosci. *Remote Sens. Lett.* 6, 122-126.

Bustos E, Meza F J (2015) A method to estimate maximum and minimum air temperature using MODIS surface temperature and vegetation data: application to the Maipo Basin, Chile. *Theoretical and Applied Climatology,* 120(1–2): 211–226. https://doi.org/10.1007/s00704-014- 1167-2.

Chen X, Zhao H, Li P and Yin Z (2006) Remote sensing image-based analysis of the relationship between urban heat island and land use/cover changes. *Remote Sensing of Environment* 104, 133–146.

Cheng X, Wei B, Chen G and Song C (2015) Influence of park size and its surrounding urban landscape patterns on the park cooling effect. *Journal of Urban Planning and Development* 141: A4014002.

Fu B, Burgher I (2015) Riparian vegetation NDVI dynamics and its relationship with climate, surface water and groundwater. *Journal of Arid Environments,* 113: 59–68. https://doi.org/10.1016/j.jaridenv.2014. 09.010.

Gao BC (1996) NDWI A normalized difference water index for remote sensing of vegetation liquid water from space. *Remote Sensing of Environment* 58, 257–266.

Jiménez-Muñoz C and Sobrino J (2003) A generalized single-channel method for retrieving land surface temperature from remote sensing data. *J. Geophys. Res*. 108.

Mimbrero M R, Vlassova L, Pé F (2014) Analysis of the Relationship between Land Surface Temperature and Wildfire Severity in a Series of Landsat Images. *Remote Sensing*, 6: 6136–6162. https://doi.org/10. 3390/rs6076136.

Qin Z, Karnieli A, and Berliner P (2001) A mono-window algorithm for retrieving land surface temperature from Landsat TM data and its application to the Israel-Egypt border region. *Int. J. Remote Sens.* 21: 3719–3746.

Qinqin Sun, Zhifeng Wu and Jianjun Tan (2012) The relationship between land surface temperature and land use/land cover in Guangzhou, China. *Environ Earth Sci* 65:1687–1694 DOI 10.1007/s12665-011-1145-2.

Rasul G, Mahmood A, Sadiq A, Khan SI (2012)Vulnerability of the Indus Delta to Climate Change in Pakistan. Pakistan Journal of Meteorology 2012; 8(16).

Sahana M, Ahmed R and Sajjad H (2016) Analyzing land surface temperature distribution in response to land use/land cover change using split window algorithm and spectral radiance model in Sundarban Biosphere Reserve, India. *Model. Earth Syst. Environ*. 2:81 DOI 10.1007/s40808-016-0135-5

Sahana M, Ahmed R and Sajjad H (2016) Analysing land surface temperature distribution in response to land use/land cover change using split window algorithm and spectral radiancemodel in Sundarban Biosphere Reserve, India. *Modeling Earth Syst. Environ*. 2.

Sobrino JA, Jimenez-Munoz JC, and Paolini L (2004) Land surface temperature retrieval from LANDSAT TM5. *Remote Sens. Environ.* 90: 434–440.

Thanh Noi Phan, Martin Kappas and Trong Phuong Tran (2018) Land Surface Temperature Variation Due to Changes in Elevation in Northwest Vietnam. *Climate*, 6, 28; doi:10.3390/cli6020028

Wedajo GB, Muleta M K, Gessesse B and Koriche SA (2019) Spatiotemporal climate and vegetation greenness changes and their nexus for Dhidhessa River Basin, Ethiopia.. *Environ Syst Res* 8:31 https://doi.org/10.1186/s40068-019-0159-8

Xu H, (2008) A new index for delineating built-up land features in satellite imagery. *International Journal of Remote Sensing* 29, 4269–4276.

Yuan F and Bauer ME (2007) Comparison of impervious surface area and normalized difference vegetation index as indicators of surface urban heat island effects in Landsat imagery. *Remote Sensing of Environment* 106, 375–386.

Zareie S, Khosravi H, Nasiri A,(2016) Using Landsat Thematic Mapper (TM) sensor to detect change in land surface temperature in relation to land use change in Yazd, Iran. *Solid Earth*, 7: 1551–1564. https://doi.org/10.5194/se-7-1551-2016.

Zha Y, Gao J and Ni S (2003) Use of normalized difference built-up index in automatically mapping urban areas from TM imagery. *International Journal of Remote Sensing* 24, 583–594.

Zhang Y, Yu T, Gu X, Zhang Y and Chen L (2006) Land surface temperature retrieval from CBERS-02 IRMSS thermal infrared data and its applications in quantitative analysis of urban heat islands effects. *J. Remote Sens.* Beijing, 10, 789.

Zhifeng Wu and Jianjun Jim Tan (2012) the relationship between land surface temperature and land use/land cover in Guangzhou, China. *Environ Earth Sci* 65:1687–1694 DOI 10.1007/s12665-011-1145-2

Zhou Xiaolu and Wang Yi-Chen (2011) Dynamics of Land Surface Temperature in Response to Land-Use/Cover Change. *Geographical Research* 49(1):23–36doi: 10.1111/j.1745-5871.2010.00686.x